Morphological and molecular recharacterization of the rodent genus *Mus* from Nepal based on museum specimens

*Makoto Kishimoto[1, *, **], Masaru Kato[2] and Hitoshi Suzuki[1]

[1]*Graduate School of Environmental Science, Hokkaido University, North 10, West 5, Sapporo 060-0810, Japan*

[2]*Field Science Center for Northern Biosphere, Botanic Garden & Museum, Hokkaido University, North 3, West 8, Sapporo, 060-0003, Japan*

Running head: Resurvey of Nepalese mouse specimens

Total number of words: 38,642 include space

*Correspondent: kishimoto@eis.hokudai.ac.jp

Abstract. The taxonomy and phylogeny of the subgenus *Mus*, the Eurasian lineage of the genus *Mus*, remain unresolved, even for the house mouse (*Mus musculus*). While the subgenus is diverse in Asia, few studies cover both its morphology and molecular phylogeny. We re-examined 70 specimens identified as *M. cervicolor* that were collected from central Nepal in 1968 and 1975 and are currently deposited in the Hokkaido University Natural History Museum. To compare morphological features, we examined skull geometric morphometrics and body coloration, and performed a phylogenetic analysis of the mitochondrial cytochrome *b* gene sequences of representative specimens. The specimens were most likely either *M. booduga* or *M. musculus*. The best morphological characteristics for distinguishing the two species were the nasal length ratio, which was high and low, respectively. *Mus booduga* was found to inhabit altitudes lower than 1000 m and have light ventral fur, while *M. musculus* inhabited various altitudes up to 3000 m and had variable fur color depending on the altitude. We also discuss the taxonomic status of the fawn-colored mouse *M. cervicolor*.

Key words: Geometric morphometrics, *Mus booduga*, *Mus cervicolor*, *Mus musculus*

The subgenus *Mus* (genus *Mus*) comprises more than 13 species distributed mainly in subtropical Eurasia (Marshall 1977; Lundrigan et al. 2002; Chevret et al. 2003; Macholán et al. 2012; Wilson et al. 2016). Based on molecular phylogenetics, the subgenus comprises four species groups roughly distributed in four geographic areas: the Mediterranean coast, India, Myanmar, and Southeast Asia (Suzuki et al. 2004; Shimada et al. 2009; Macholán et al. 2012). The high diversity of color and shape within and among species makes classification difficult, even for the house mouse (*Mus musculus*).

Morphological diversity is important when evaluating environmental and genetic factors. Because of its diverse environment, Nepal is a hotspot of morphological and genetic differentiation of mammals (Baral and Shah 2008; Pearch 2011), and detailed surveys in this area could provide important information. There are many reports on small rodents in Nepal (e.g., Michael 1981; Thapa 2014; Prakash et al. 2015), but few have used both molecular and morphological methods (Adhikari et al. 2018a, b).

One of the least understood species in Nepal is the fawn-colored mouse (*M. cervicolor*). This name was first given to mice collected in Nepal by Hodgson (1845). The species was thought to occur over a wide area from Nepal to Southeast Asia, including Myanmar, but its range is still debated (Marshall 1977; Macholán et al. 2012; Aplin and Molur 2016) (Fig. 1A). Specimens from Thailand have been used as a reference for *M. cervicolor* in molecular phylogenetic analyses (Lundrigan et al., 2002; Suzuki et al. 2004; Shimada et al. 2009). However, some specimens from Myanmar and Cambodia were ultimately found to be other species (*M. nitidulus* and *M. fragilicauda*), which have similar morphological traits (Suzuki et al. 2004; Shimada et al. 2007; Myat

Myat Zaw et al. 2019). This suggests the need to re-characterize the species *M. cervicolor* based on specimens from Nepal, its original locality.

Skull geometric morphometrics (GM) of *Mus* specimens have been used to study the phenotypes of species in Europe (Macholán 2001; Macholán et al. 2008; Siahsarvie et al. 2012; Hamid et al. 2017). This method can discriminate related species of *Mus* from Europe (Macholán 2001; Macholán et al. 2008) and does not destroy museum specimens.

Morphological and molecular analysis of specimens from Nepal can provide valuable insight into the distribution of *Mus*, and its geography and ecology. Here, we revalidate specimens previously identified as *M. cervicolor* from Nepal based on their morphology, including skull GM and body coloration, and conduct a phylogenetic analysis based on the mitochondorial cytochrome *b* (*Cytb*) region.

Materials and methods

Mouse specimens

We examined the flat skins and skulls of 70 mice collected from 15 sites in central Nepal (Fig. 1B, Table 1) by H. Abe of the Hokkaido University Himalayan Committee in 1968 and 1975, and stored in the Hokkaido University Natural History Museum (HUNHM) (HUNHM 57325–57394, $n = 70$; hereafter, the Abe Collection) (Abe 1971, 1977; Abe and Kato 2014, 2015). Abe (1971, 1977) identified all of the specimens as *M. c. cervicolor* or *M. c. phillipsi* based on Ellerman (1961). Here, we identified all specimens as adults based on erupted third upper molars (Siahsarvie et al. 2012). Specimens of both sexes were pooled since no significant sexual dimorphism has been reported in murine rodents (Renaud 2005). As references in some analyses, we

used 19 *M. musculus*, two *M. booduga*, two *M. caroli*, and three *M. cookii* from Asian sites stored at HUNHM (Table 2).

Morphological analyses

We analyzed the skull morphology using the traditional method and GM. The traditional method uses 16 cranial and six dental measurements (Fig. 2) (cf. Ellerman 1961; Marshall 1977; Agrawal 2000). Each skull was measured three times to the nearest 0.01 mm using digital calipers and the average values were used in the analyses. We also used three external measurements recorded on the labels by Abe (Ellerman 1947, 1961; Marshall 1977; Agrawal 2000): body and head length (B+H), tail length (TL), and hindfoot length (HL). The GM approach focuses on shape, and uses landmark points plotted on images (Rohlf and Marcus 1993). The simplest landmarks were used to include as many individuals as possible. The Cartesian coordinates of each landmark were compared and the enlarged or reduced regions relative to others were shown as the expansion or contraction in grids. Images of the dorsal surfaces of skulls (n = 59) were captured by adjusting the occlusal surface of the skull to be as horizontal as possible. We selected 14 landmarks and digitized only the left side to rule out any possible influence of asymmetry (Macholán et al. 2008) (Fig. 3). The coordinates of each landmark were captured using tpsDIG software (ver. 2.30; Rohlf, 2017) and all landmarks were superimposed using the full or partial Procrustes fit, performed with MorphoJ software (ver. 1.06d; Klingenberg 2011).

Ventral body color was quantified with a spectrophotometer (CM-700d/CM-600d; Konica Minolta, Osaka, Japan) with the specular component included (SCI). Five ventral areas (middle, near head, near tail, right side, and left side) were measured and

the average scores were used in the analysis (Supplementary material 1). CIELAB color space (L*a*b*) was used (L*, luminosity from black to white [0, 100]; a*, color from green to red [–60, 60]; b*, color from blue to yellow [–60, 60]).

Data analyses

In the GM analysis, to assess variation in skull shape based on landmark configuration, principal component analysis (PCA) was conducted in MorphoJ using the Procrustes fit. We used k-means and gap statistics for non-hierarchical cluster analyses based on PCA scores to determine the appropriate number of groups and group members (1000 bootstraps). The best centroid coordinate and group members are calculated by k-means in each cluster number. And the best centroid makes the lowest G (k) (k is the number of cluster) that means the sum of the pairwise distances between each points and centroid. Then Gap (k) is calculated as G (k) – G (k + 1) and means the effect of increasing of the cluster number. The best cluster number makes the biggest jump into a reduced total-cluster distance by introducing a new centroid. So the k that maximizes Gap (k) is the best number of clusters. We conducted canonical variance analysis (CVA) using the Procrustes fit, analysis of variance (ANOVA) of centroid size (CS), and Procrustes ANOVA to validate the groupings. These analyses were also performed in MorphoJ. CS was calculated as the sum of the distances between centroids (center of gravity).

We applied four indexes: B+H/TL, nasal length (NL) – greatest length of skull (GLS)/4, GLS/cranial width (CW), and NL/GLS. Regression analysis was performed in R software (ver. 3. 4. 0; R Development Core Team 2017), including all of the indexes. We only included specimens with all measurement values (n = 59) in the analysis.

Molecular analyses

Instead of destructive sampling, 25 specimens selected from the Abe Collection (based on their morphological characteristics and collection sites) were subjected to molecular analysis. We removed a single toe of a hind foot and preserved it in 100% EtOH. DNA was extracted using a DNA Investigator Kit (Qiagen, Hilden, Germany). The specimens were shredded mechanically and incubated with lysis buffer containing proteinase K for 4 h at 55°C. Polymerase chain reaction (PCR) and direct sequencing of the mitochondrial *Cytb* were performed as described previously (Suzuki et al. 2004, 2013; Yasuda et al. 2005) using AmpliTaq Gold 360 DNA polymerase (Invitrogen, Carlsbad, CA, USA). We designed the following primers for *Mus* genes: upper (*Cytb*_L1, 5'-GACATGAAAAATCATCGTTG-3'; *Cytb*_R1, 5'-GATTGTATAGTAGGGATGAAATGG-3') and lower (*Cytb*_L2, 5'-CCTATCAGCCATCCCATATATTGG-3'; *Cytb*_R2, 5'-GTTTACAAGACCAGAGTAAT-3') and two short regions (*Cytb*_L3, 5'-GGCTACGTCCTTCCATGAGG-3'; *Cytb*_R3, 5'-GGGTTGTTTGATCCTGTTTCGTG-3' and *Cytb*_L4, 5'-CCTTGACCCGATTCTTCGCT-3'; *Cytb*_R4, 5'-AGGCTTCGTTGCTTTGAGGT-3'). An initial step of 95°C for 10 min was followed by 35 cycles of 95°C for 30 s, 50°C for 30 s, and 60°C for 30 s. The double-stranded PCR product was purified using 20% polyethylene glycol–2.5 M NaCl precipitation and sequenced directly using a BigDye Terminator Cycle Sequencing Kit and ABI 3130 (Applied Biosystems, Foster City, CA, USA), according to the manufacturer's instructions. The sequences were analyzed at least twice in each region

and only those that were reproducible were included in the final analysis (n = 17). Sequence alignment and phylogenetic trees of the mtDNA sequences were constructed using the maximum likelihood (ML) method with MEGA7 (Kumar et al. 2016). The reliability of the nodes was assessed using 1000 bootstraps. The Hasegawa–Kishino–Yano (HKY)+G+I model was selected as the best model based on the corrected Akaike information criterion (AICc) and Bayesian information criterion (BIC) scores. All sequences have been deposited in the DDBJ, EMBL, and GenBank databases under accession numbers LC455566–LC455570 and LC605035–LC605046 (Table 1). We used 26 *Mus* sequences (1140 bp) as the ingroup and reference sequences from GenBank.

Results

Morphological analyses

We used morphological measurements to identify the 70 mice from the Abe Collection to species using the criteria of Marshall (1977), and found that we were able to separate them, but the results were indecipherable, as they were divided into several species (data not shown).

In the GM analysis, Gap (k) was highest when there were three clusters (Fig. 4). Three clusters consist of 12 (Group I), 23 (Group II), and 24 (Group III) specimens (Table 1). In CVA with the Procrustes fit, both the Mahalanobis and Procrustes distances were significantly different between groups ($P < 0.001$). In the ANOVA and Procrustes ANOVA, CS and shape differed significantly between groups (both $P < 0.001$) (Supplementary material 2). The amount of between-group variance explained by seven PC axes was 40.3%, 11.5%, 8.9%, 6.6%, 5.7%, 4.9%, and 4.1% for

PC 1–7, respectively. Figure 5 shows the morphological variation described by the first two principal components. PC1 corresponds to the length of the rostral part and lateral width of the occiput. We found differences among Groups I–III. Groups I and III had the smallest and largest PC1, respectively. In the scatterplots between PC1 and PC2, Groups II and III overlapped, but neither overlapped with Group I.

Molecular analyses

From the three skull groups, we obtained long *Cytb* sequences for 12 specimens (600–1140 bp) and short sequences for five others (ca. 200 bp, primer pairs of L3 and H3). We constructed a ML tree with the 17 readable sequences, and reference sequences of the subgenus *Mus* and found that our Nepalese sequences were integrated into either the *M. musculus* or *M. booduga* species cluster (Fig. 6). All three skull groups were present in both clusters: *M. musculus* (Groups I –III, n = 3, 4, and 4, respectively) and *M. booduga* (Groups I–III, n = 1, 1, and 3, respectively). Our results showed that the haplotypes of mice in the Abe Collection had no specific phylogenetic relationships with those of other species of the subgenus *Mus*, including *M. cervicolor*.

Ventral coloration and elevation

We analyzed the correlations among the L*, a*, and b* values, obtained spectrophotometrically, as well as their correlations with elevation. The L* values were correlated with elevation (R^2 = 0.67, Fig. 7). The a* and b* values were little correlated with each other (R^2 = 0.38), but neither was correlated with elevation (R^2 = 0.05 and R^2 = 0.01, respectively). Groups I and II had lower L* values (dark coloration) and were distributed at higher elevations (R^2 = 0.61 and R^2 = 0.63, respectively), while Group III

individuals had higher L* values (whitish color) and were distributed at lower elevations ($R^2 = 0.83$). Ventral coloration and elevation were correlated in specimens identified as *M. musculus* ($R^2 = 0.63$), but not in *M. booduga* ($R^2 = 0.32$).

Index values

We compared the mean values for the various indexes among the groups. ANOVA based on GM revealed significant group differences in GLS, NL, L, NL – GLS/4, GLS/CW, NL/GLS, and CS ($P < 0.001$). According to the Tukey–Kramer *post hoc* test, the group differences in L*, NL – GLS/4, and NL/GLS were attributable to those between Groups I and II versus Group III. Table 2 shows the index values. In the GM analysis, the GLS was lowest in Group I, while Groups II and III had similar values. The NL was lowest in Group I and highest in Group III. The NL/GLS ratio was highest in Group III (Table 2), in line with PC1 in the GM analysis. In the GM analysis of the Abe Collection, elevation and GLS were correlated only in Group II ($R^2 = 0.53$). In the partial genetic analysis, *M. booduga* from the Abe Collection had similar mean GLS and NL/GLS values between Groups II and III (Table 2), and the GLS of four of the five specimens exceeded 20 mm. These values differed from those of *M. booduga* in outgroup. There was no correlation between elevation and skull size. Therefore, *M. booduga* in the Abe Collection (Group III) were larger in terms of skull and body size than Indian *M. booduga*, but had a similar snout ratio. Similarly, the GLS of the *M. musculus* outgroup was 20.04 mm ± 1.3, and the snout ratio was 0.35 ($n = 19$), similar to *M. musculus* in the Abe Collection (Groups I and II).

Discussion

Correspondence of the morphological and molecular analyses

Responses to the environment differ by species and region, which makes it challenging to understand the morphological variation in *Mus*. Previous studies of small rodents reported island gigantism, with some species following Bergman's rule (Macholán et al. 2008; Cui et al. 2020). Here, we examined museum specimens collected in central Nepal, at elevations of 300 to 3200 m, which were previously identified as *M. cervicolor* (*n* = 70) (Abe 1971, 1977). We found substantial variation in the skull morphology among specimens from Nepal, which were divided into three groups using gap statistics and k-means clustering, based on PCA of the Procrustes fit (Fig. 4). Group I had a short snout and wide lateral occiput; Group III had a long snout and narrow occiput; and Group II was intermediate between Groups I and III (Fig. 5, Table 2). Moreover, light ventral coloration (i.e., high L* value) and elevation were associated, with darker fur seen at higher elevations (Fig. 7). Groups I and II tended to have darker fur than Group III (Fig. 7). We analyzed sequence data and found that 12 (600–1140 bp) and five (200 bp) specimens had sequence clusters corresponding to *M. musculus* and *M. booduga* (Fig. 6), respectively, based on the skull morphology, ventral fur color, and elevational distribution (Fig. 7). Considering these findings and the NL ratios of the reference specimens of *M. booduga* (*n* = 2) and *M. musculus* (*n* = 19, Table 2), we concluded that Groups I and II could be assigned to be *M. musculus* and Group III to *M. booduga*, although there were some exceptions. *Mus booduga* has a long snout and pure white ventral coat, and is commonly found in the Indian subcontinent and at low elevations in southern Nepal (Terai region), while *M. musculus* tends to co-occur with humans and has variable fur color (Aplin and Molur 2016).

A small GLS (18–20 mm) is an important reference characteristic for *M. booduga* (Macholán et al. 2012); the GLS was 21.09 ± 1.54 for *M. booduga* in the Abe Collection (Table 2). Abe (1977) identified the specimens as *M. cervicolor* and categorized them into two subspecies based on the elevation of the collection sites (above or below 1000 m). He described *M. c. phillipsi* distributed at low altitudes as having a long snout, white ventral coat, and teeth like *M. booduga*. He identified them as *M. cervicolor* because they were too large to be *M. booduga* compared to the Indian specimens. Our results suggest that the skull size increased in *M. booduga* in Nepal, while the snout ratio did not change (Table 2). While the snout ratio is a species characteristic (Aplin and Molur 2016), the skull size might be explained by environmental factors, such as the presence of closely related species (e.g., *M. musculus*). Two exceptions had a small GLS (HUNHM57389, 19.02 mm; HUNHM57330, 20.09 mm; Table 1 and Fig. 5), so they might have been relatively young individuals with incomplete rostral development. In summary, we are able to identify the species via GM analysis in the majority of specimens. To improve species identification, other point selection methods may be useful, such as using three-dimensional and semi-landmarks. Alternatively, other body parts such as the mandible, and other landmark positions, may facilitate classification.

Abe (1982) noted an elevational shift in vegetation in his study area in central Nepal, which comprised cultivated fields and tropical broad-leaved forests in Terai, cultivated open areas at 1000–2600 m, and shrub (Rhododendron) and coniferous forests above 2600 m. The Group I and II specimens assigned as *M. musculus* were collected at both low and high elevations, ranging from 300–3200 m, probably due to its cohabitation with humans. At high elevations in Nepal, only *M. musculus* was thought

to occur. However, Abe collected *M. booduga* at elevations less than 1150 m above sea level. In India, *M. booduga* is reported to occur in croplands at high elevation (3768 m; Chaudhary and Tripathi 2018). Therefore, more ecological research is needed.

In this study, there were clear differences in the ventral fur color and habitat preference within and between species (Fig. 7). These tendencies are consistent with previous studies (Agrawal 2000; Macholán et al. 2012; Adhikari et al. 2018b). Lai et al. (2008) reported a relationship between fur color and soil conditions; for example, dark fur color was associated with high humidity in *M. musculus*. Lai et al. (2008) reported a relationship between fur color and soil conditions; for example, dark fur color was associated with high humidity in M. musculus. Counter-shading may also be able to explain the observed ventral fur color difference. In this study, HUNHM57386, assigned as *M. musculus* and collected at low elevations, had a white ventral surface, and a fur color pattern similar to *M. booduga* collected at elevations lower than 1150 m (Fig. 7). This may suggest the morphological change depending on the habitat environment. Nepalese mice are suitable for studying the evolutionary basis of ventral coat color diversity (Adhikari et al. 2018b; this study), which is controlled by specific genes (e.g., Sakuma et al. 2019).

The overlapping morphological features observed in *M. booduga* and *M. musculus* from Nepal can be explained either by ecotype adaptation to a heterogeneous environment (e.g., in terms of elevation) or admixing of phylogenetically distinct groups (i.e., subspecies) that merged in Nepal. To better understand this, mtDNA genotyping and nuclear markers are needed. Elevation is not the only relevant environmental factor; competition and the food supply could also drive differentiation (Kamilar 2009; Singh et al. 2009). Further studies should examine the specific factors that promote

differentiation. Our study showed the importance of the nasal ratio and ventral coloration for distinguishing *M. musculus* and *M. booduga* in Nepal, whereas a small skull could not distinguish *M. booduga* in Nepal.

Genetic diversity in Mus musculus from Nepal

Prager et al. (1998) revealed the presence of unique mitochondrial control region haplotypes in Nepal. One of the five major mtDNA lineages of *M. musculus* was reported to exist exclusively in Nepal (tentatively called "NEP") (Terashima et al. 2006; Suzuki et al. 2013; Sakuma et al. 2016; Li et al. 2020). Adhikari et al. (2018b) reported two distinct sublineages of *M. m. castaneus*, labeled as "*M. m. bactrianus*" and "*M. m. castaneus*". Hence, the phylogenetic status of *M. musculus* from Nepal remains unclear, partly due to a lack of morphological analyses. Whereas we found substantial morphological variation in the Abe Collection of *M. musculus*, as reflected in the difference between Groups I and II, mtDNA sequence analysis did not reveal any differences, largely due to the short *Cytb* segment analyzed. Molecular phylogenetic analyses should be conducted to study the genetic diversity of mice in Nepal, which will allow us to determine the taxonomic position of the Nepalese mice.

Distribution of M. cervicolor

The molecular analysis did not support the inclusion of *M. cervicolor* in the Abe Collection (Fig. 6). Hodgson (1845) described two field mouse taxa from Nepal, i.e., *M. cervicolor* and *M. strophiatus*, although subsequent researchers have treated them as a single species; Ellerman (1961) considered the combined taxa the typical species in

Nepal. However, Marshall (1977) re-examined museum and newly collected specimens from Nepal, and designated *M. cervicolor* based on the proodont incisor shape.

Many researchers have questioned the broad distribution of *M. cervicolor* from Nepal to Vietnam (Fig. 1A; Marshall 1977; Macholán et al. 2012; Aplin and Molur 2016). We examined Marshall's (1977) morphological characters, including incisor shape, but did not find any *M. cervicolor* specimens (data not shown), suggesting that it is less abundant in Nepal. Thus, *M. cervicolor* specimens identified before 1977, such as those in the Abe Collection, would likely be considered as different species based on our criteria. Hodgson (1845) described one of the two original species (*M. strophiatus*) as having a pure white ventral coat, suggesting that his specimens included large *M. booduga*. Molecular analysis showed that *M. cervicolor* in Thailand is closely related to *M. cookii* and *M. caroli* in Southeast Asia (Chevret et al. 2003; Shimada et al. 2009). In their molecular analyses, Auffray et al. (2003) identified a distinct species in Thailand (*M. fragilicauda*). A morphological and molecular survey of *Mus* in Myanmar revealed a unique lineage that was previously recognized as *M. cervicolor*, but has since been renamed *M. nitidulus* (Shimada et al. 2007). A broad survey of *Mus* in Myanmar revealed that *M. nitidulus* is common (Myat Myat Zaw et al. 2019), in turn implying that *M. cervicolor* is absent in Myanmar. These new molecular analyses suggest the difficulty of species identification based on morphological characteristics, partly because the species divergence is not ancient and they share similar ecological features. It is conceivable that the *Mus* taxon from Thailand has been incorrectly identified as *M. cervicolor*. A careful study of the type specimen of *M. cervicolor* from Nepal, and of the taxon currently treated as *M. cervicolor* from Thailand, is needed, along with a thorough survey of Nepalese rodents.

Acknowledgments

We thank Hisashi Abe, Kimiyuki Tsuchiya, and Fumihito Takaya for access to the collection. John Bower helped edit the English in the manuscript. We also thank Associate Editor Masaharu Motokawa and three reviewers for their valuable comments on the manuscript. This study was supported by a Grant-in-Aid for Scientific Research on Innovative Areas to HS (JS18H05508).

References

Abe, H. 1971. Small mammals of central Nepal. Journal of the Faculty of Agriculture 56: 367–423.

Abe, H. 1977. Variation and taxonomy of some small mammals from central Nepal. Journal of the Mammalogical Society of Japan 7: 63–73.

Abe, H. 1982. Ecological distribution and faunal structure of small mammals in central Nepal. Mammalia 46: 477–504.

Abe, H. and Kato, M. 2014. Hokkaido University Central Nepal Biological Survey Team Research Handbook (1968) by Abe Hisashi. Bulletin of Botanic Garden, Hokkaido University 14: 53–85 (in Japanese).

Abe, H. and Kato, M. 2015. Hokkaido University Central Nepal Biological Survey Team Research Handbook (1975) by Abe Hisashi. Bulletin of Botanic Garden, Hokkaido University 15: 55–70 (in Japanese).

Adhikari, P., Han, S. H., Kim, Y. K., Kim, T. W., Thapa, T. B., Subedi, N., Adhikari, P. and Oh, H. S. 2018b. First molecular evidence of *Mus musculus bactrianus* in Nepal inferred from the mitochondrial DNA *cytochrome B* gene sequences. Mitochondrial DNA Part A 29: 561–566.

Adhikari, P., Han, S. H., Kim, Y. K., Kim, T. W., Thapa, T. B., Subedi, N., Kunwar, A., Banjade, M. and Oh, H. S. 2018a. New record of the Oriental house rat, *Rattus tanezumi*, in Nepal inferred from mitochondrial *Cytochrome B* gene sequences. Mitochondrial DNA Part B 3: 386–390.

Agrawal, V. C. 2000. Taxonomic Studies on Indian Muridae and Hystricidae (Mammalia: Rodentia). Zoological Survey of India, Kolkata, 177 pp.

Aplin, K. and Molur, S. 2016. *Mus cervicolor*. The IUCN Red List of Threatened Species 2016: e.T13957A22403025. https://dx.doi.org/10.2305/IUCN.UK.2016-2.RLTS.T13957A22403025.en (Accessed 9 February 2021).

Auffray, J. C., Orth, A., Catalan, J., Gonzalez, J.-P., Desmarais, E. and Bonhomme, F. 2003. Phylogenetic position and description of a new species of subgenus *Mus* (Rodentia, Mammalia) from Thailand. Zoologica Scripta 32: 119–127.

Baral, H. S. and Shah, K. B. 2008. Wild Mammals of Nepal. Himalayan Nature, Kathmandu, 188 pp.

Chaudhary, V. and Tripathi, R. S. 2018. First record of Little Indian field mouse, *Mus booduga* (Gray 1837) (Rodentia: Muridae), from cold arid region of Leh-Ladakh, Jammu and Kashmir, India. Mammalia 83: 97–99.

Chevret, P., Jenkins, P. and Catzeflis, F. 2003. Evolutionary systematics of the Indian mouse *Mus famulus* Bonhote, 1898: molecular (DNA/DNA hybridization and 12S rRNA sequences) and morphological evidence. Zoological Journal of the Linnean Society 137: 385–401.

Cui, J., Wang, B., Ji, S., Su, H. and Zhou, Y. 2020. Revisiting classic ecogeographical rules, using a widely distributed mouse species (*Apodemus draco*). Animal Biology 70: 359–372.

Ellerman, J. R. 1947. A key to the rodentia inhabiting India, Ceylon, and Burma (based on collections in the British Museum) Part II. Journal of Mammalogy 28: 357–387.

Ellerman, J. R. 1961. The Fauna of India Including Pakistan, Burma and Ceylon: Mammalia, Rodentia. vol. 3 (in 2 parts). vol. 1. Second edition. Zoological Survey of India, Calcutta, 482 pp.

Hamid, H. S., Darvish, J., Rastegar-Pouyani, E. and Mahmoudi, A. 2017. Subspecies differentiation of the house mouse *Mus musculus* Linnaeus, 1758 in the center and east of the Iranian plateau and Afghanistan. Mammalia 81: 147–168.

Hodgson, B. H. 1845. On the rats, mice, and shrews of the central region of Nepal. Annals and Magazine of Natural History 15: 266–270.

Kamilar, J. M. 2009. Interspecific variation in primate countershading: Effects of activity pattern, body mass, and phylogeny. International Journal of Primatology 30: 877–891.

Klingenberg, C. P. 2011. MorphoJ: An Integrated Software Package for Geometric Morphometrics. Available at https://morphometrics.uk/MorphoJ_page.html (Accessed 9 February 2021).

Kumar, S., Stecher, G. and Tamura, K. 2016. MEGA7. Available at https://www.megasoftware.net/ (Accessed 26 May 2021).

Lai, Y. C., Shiroishi, T., Moriwaki, K., Motokawa, M. and Yu, H. T. 2008. Variation of coat color in house mice throughout Asia. Journal of Zoology 274: 270–276.

Li, Y., Fujiwara, K., Osada, N., Kawai, Y., Takada, T., Kryukov, A. P., Abe, K., Yonekawa, H., Shiroishi, T., Moriwaki, K., et al. 2020. House mouse *Mus musculus* dispersal in East Eurasia inferred from 98 newly determined complete mitochondrial genome sequences. Heredity 126: 132–147.

Lundrigan, B. L., Jasa, S. A., Tucker, P. K. and Sullivan, J. 2002. Phylogenetic relationships in the genus *Mus*, based on paternally, maternally, and biparentally inherited characters. Systematic Biology 51: 410–431.

Macholán, M. 2001. Multivariate analysis of morphometric variation in Asian *Mus* and Sub-Saharan *Nannomys* (Rodentia: Muridae). Zoologischer Anzeiger - A Journal of Comparative Zoology 240: 7–14.

Macholán, M., Baird, S. J., Piálek, J. and Munclinger, P. 2012. Evolution of the House Mouse. Cambridge University Press, Cambridge, 548 pp.

Macholán, M., Mikula, O. and Vohralik, V. 2008. Geographic phenetic variation of two eastern-Mediterranean non-commensal mouse species, *Mus* macedonicus and *M. cypriacus* (Rodentia: Muridae) based on traditional and geometric approaches to

morphometrics. Zoologischer Anzeiger - A Journal of Comparative Zoology 247: 67–80.

Marshall, J. T. 1977. A synopsis of Asian species of *Mus* (Rodentia, Muridae). Bulletin American Museum of Natural History 158: 173–220.

Michael, J. B. G. 1981. A check-list and some notes concerning the mammals of the Langtang national park, Nepal. The Journal of the Bombay Natural History Society 78: 77–87.

Myat Myat Zaw, K., Thwe, T., Shimada, T., Maung Maung Theint, S., Saing, K. M., Bawm, S., Katakura, K. and Suzuki, H. 2019. Molecular characterization of species of the subgenus *Mus* from Myanmar. Zoological Science 36: 299–305.

Pearch, M. J. 2011. A review of the biological diversity and distribution of small mammal taxa in the terrestrial ecoregions and protected areas of Nepal. Zootaxa 3072: 1–286.

Prager, E. M., Orrego, C. and Sage, R. D. 1998. Genetic variation and phylogeography of central Asian and other house mice, including a major new mitochondrial lineage in Yemen. Genetics 150: 835–861.

Prakash, I., Singh, P., Nameer, P., Ramesh, D. and Molur, S. 2015. South asian muroids. Mammals of South Asia 2: 574–642.

R Core Team 2017. R: A Language and Environment for Statistical Computing. R Foundation for Statistical Computing, Vienna, Austria. Available at https://www.R-project.org/ (Accessed 9 May 2021).

Renaud, S. 2005. First upper molar and mandible shape of wood mice (*Apodemus sylvaticus*) from northern Germany: Ageing, habitat and insularity. Mammalian Biology 70: 157–170.

Rohlf, F. 2017. tpsDig2, version 2.30. TpsSeries. Available at http://www.sbmorphometrics.org/soft-dataacq.html/ (Accessed 26 May 2021).

Rohlf, F. and Marcus, L. F. 1993. A revolution in morphometrics. Trends in Ecology & Evolution 8: 129–132.

Sakuma, Y., Matsunami, M., Takada, T. and Suzuki, H. 2019. Multiple conserved elements structuring inverted repeats in the mammalian coat color-related gene *Asip*. Zoological Science 36: 23–30.

Sakuma, Y., Ranorosoa, M. C., Kinoshita, G., Shimoji, H., Tsuchiya, K., Ohdachi, S. D., Arai, S., Tanaka, C., Ramino, H. and Suzuki, H. 2016. Variation in the coat-color-controlling genes, *Mc1r* and *Asip*, in the house mouse *Mus musculus* from Madagascar. Mammal Study 41: 131–140.

Shimada, T., Aplin, K. P., Jenkins, P. and Suzuki, H. 2007. Rediscovery of *Mus nitidulus* Blyth (rodentia: Muridae), an endemic murine rodent of the central basin of Myanmar. Zootaxa 68: 45–68.

Shimada, T., Sato, J. J., Aplin, K. P. and Suzuki, H. 2009. Comparative analysis of evolutionary modes in *Mc1r* coat color gene in wild mice and mustelids. Genes & Genetic Systems 84: 225–231.

Siahsarvie, R., Auffray, J. C., Darvish, J., Rajabi-Maham, H., Yu, H. T., Agret, S., Bonhomme, F. and Claude, J. 2012. Patterns of morphological evolution in the mandible of the house mouse *Mus musculus* (Rodentia: Muridae). Biological Journal of the Linnean Society 105: 635–647.

Singh, S., Cheong, N., Narayan, G. and Sharma, T. 2009. Burrow characteristics of the co-existing sibling species *Mus booduga* and *Mus terricolor* and the genetic basis of adaptation to hypoxic/hypercapnic stress. BMC Ecology 9: 1–7.

Suzuki, H., Nunome, M., Kinoshita, G., Aplin, K. P., Vogel, P., Kryukov, A. P., Jin, M. L., Han, S. H., Maryanto, I., Tsuchiya, K., et al. 2013. Evolutionary and dispersal history of Eurasian house mice *Mus musculus* clarified by more extensive geographic sampling of mitochondrial DNA. Heredity 111: 375–390.

Suzuki, H., Shimada, T., Terashima, M., Tsuchiya, K. and Aplin, K. 2004. Temporal, spatial, and ecological modes of evolution of Eurasian *Mus* based on mitochondrial and nuclear gene sequences. Molecular Phylogenetics and Evolution 33: 626–646.

Terashima, M., Furusawa, S., Hanzawa, N., Tsuchiya, K., Suyanto, A., Moriwaki, K., Yonekawa, H. and Suzuki, H. 2006. Phylogeographic origin of Hokkaido house mice (*Mus musculus*) as indicated by genetic markers with maternal, paternal and biparental inheritance. Heredity 96: 128–138.

Thapa, S. 2014. A checklist of mammals of Nepal. Journal of Threatened Taxa 6: 6061–6072.

Wilson, D. E., Lacher, T. E. and Mittermeier, R. A. 2016. Handbook of the Mammals of the World, Volume 6: Lagomorphs and Rodents I. Lynx Edicions, Barcelona, 987 pp.

Yasuda, S. P., Vogei, P., Tsuchiya, K., Han, S. H., Lin, L. K. and Suzuki, H. 2005. Phylogeographic patterning of mtDNA in the widely distributed harvest mouse (*Micromys minutus*) suggests dramatic cycles of range contraction and expansion during the mid- to late Pleistocene. Canadian Journal of Zoology 83: 1411–1420.

Figure Legends

Figure 1. Distribution of *Mus cervicolor* and a map of the collection sites in central Nepal. **A**) The gray area shows the distribution of *M. cervicolor* according to Macholán et al. (2012). **B**) Three circles (black, gray, and white) and a cross shown in each collection site mean different groups demarcated by the GM analysis; Group I, black circles; Group II, gray circles; Group III, open circles; unparsed in the GM analysis, crosses (Table 1). The details of the collection sites are provided in Abe (1971, 1977) and Abe and Kato (2014, 2015).

Figure 2. Traditional cranial measurements for *Mus*. BL, bulla length; BW, bulla width; CW, cranial width; DL, diastema length; DW, dentition width; GLS, great length of skull; IFL, incisive foramina length; IPSW, interpterygoid space width; IPSL, interpterygoid space length; IW, interorbital width; LD, length of dentition; M1, molar 1 length; M1W, molars 1 width; ML', mandible length; MW, molar width; NL, nasal length; NW, nasal width; ORB, orbital length; ORBW, orbital width; PL, palate length; RD, rostrum depth; RL, rostrum length (Ellerman 1947, 1961; Marshall 1977; Agrawal 2000).

Figure 3. Distal side of the mouse skull (right) and landmark positions (dots) (left) following Macholán et al. (2008). 1, rostral-most point of the nasal bone (rhinion); 2, intersection of the naso-frontal suture in the midline (nasion); 3, intersection of the coronal and sagittal sutures (bregma); 4, intersection of the sagittal and parietal-interparietal sutures (lambda); 5, caudal end of the curvature of the occipital (opistocranion); 6, intersection of the rostral curvature of the nasal process of the

incisive bone (Processus nasalis ossis incisivi) and the nasal bone in the dorsal projection; 7, point of maximum curvature of the rostro-lateral part of the maxilla; 8, rostral end of the zygomatic plate; 9, caudal end of the intersection of the zygomatic process of the maxilla and the upper limb of this process; 10, lateral end of the naso-frontal suture in the dorsal projection; 11, rostral-most point of the parietal bone; 12, rostral end of the zygomatic process of the temporal bone (Processus zygomaticus partis squamosae ossis temporalis); 13, intersection of the parietal-interparietal and interparietal-occipital sutures; 14, caudo-lateral end of the occipital bone in the dorsal projection.

Figure 4. Optimal numbers of clusters obtained using the clusGap function, and a goodness of clustering measure with 1000 bootstraps (gap statistics performed in R). The maximum number of clusters was set at five. We chose *k* as the number of clusters such that maximize Gap (*k*).

Figure 5. Scatterplot of the first two principal components (*n* = 59, landmark number = 14) reflecting the groupings based on k-means clustering, gap statistics and the results of the molecular analysis. The top left and bottom figures are deformation grids. Group I, black circles; Group II, gray circles; Group III, open circles. HUNHM specimen numbers are shown for the specimens for which *Cytb* sequences were analyzed. Black tag, *Mus musculus*; white tag, *M. booduga*. At the bottom and left, thin-plate spline deformation grids correspond to +0.02 (black line) and –0.06 (gray line) displacements along the first PC axis and +0.02 (black line) and –0.04 (gray line) were applied to second PC axis.

Figure 6. Maximum likelihood tree based on the mtDNA *Cytb* sequences of 17 specimens from the Abe Collection and reference sequences of various species (*Mus musculus*, *M. booduga*, *M. cervicolor*, *M. platythrix*, and *M. lepidoides*). The tree is drawn to scale, with branch lengths indicating the number of substitutions per site. Bootstrap values over 50 are shown. Group I, black circles; Group II, gray circles; Group III, open circles.

Figure 7. Scatterplot of the elevation (m) of collecting sites versus the L* values of the ventral surface from samples in the Abe Collection (n = 59). Group I, black circles; Group II, gray circles; Group III, open circles; unparsed in the GM analysis, cross. The HUNHM numbers of specimens with *Cytb* sequences are shown. Black tag, *Mus musculus*; white tag, *M. booduga*.

Appendix

Supplementary material 1. Images of *Mus* skins from the ventral and dorsal sides.

Supplementary material 2. The results of ANOVA and Procrustes ANOVA of the shape Cartesian coordinates based on the PCA of the Abe Collection. The results of CVA of the Mahalanobis and Procrustes distances.

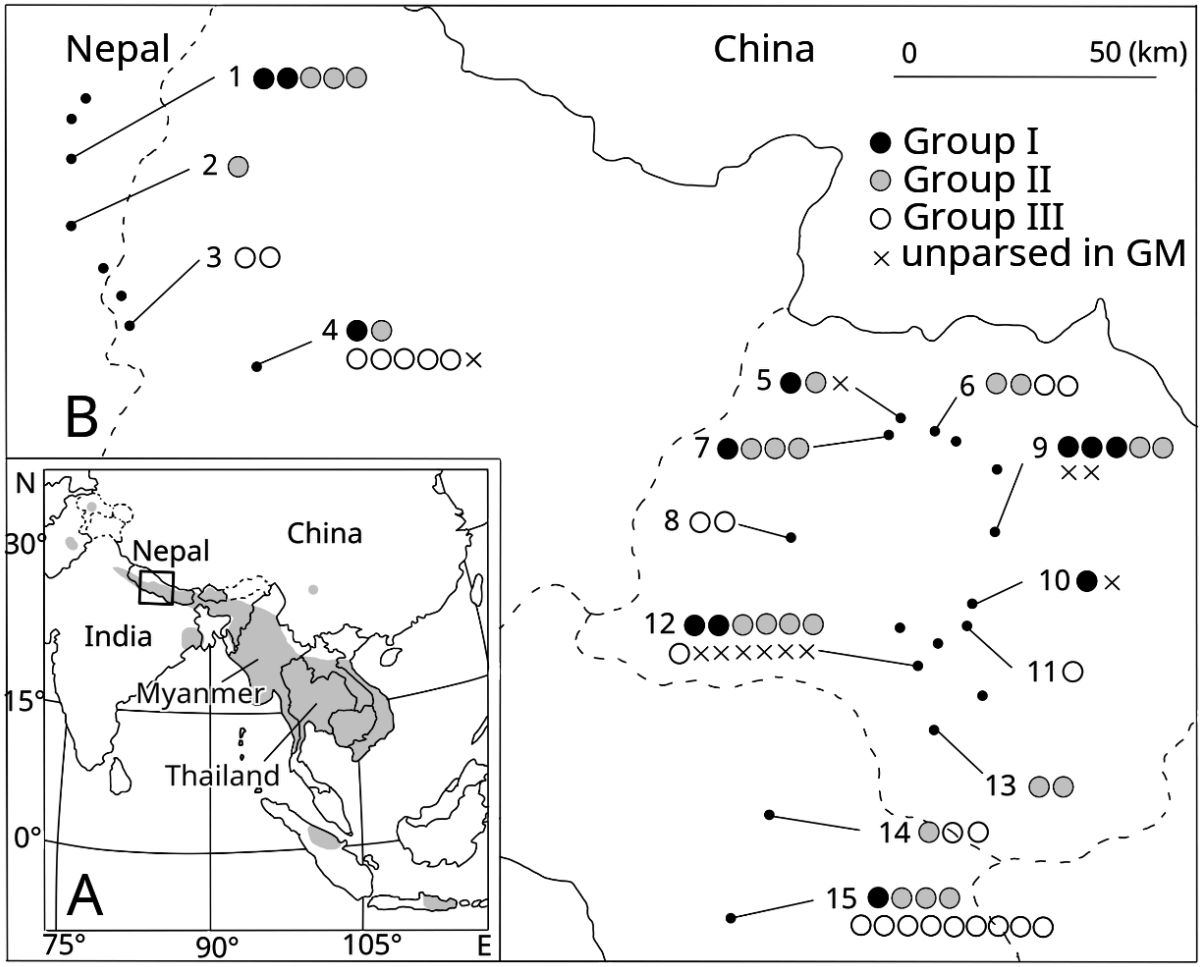
Nepal
China
0
50 (km)
Group I
Group II
Group III
unparsed in GM
B
A
N
30°
15°
0°
75°
90°
105°
E
Nepal
China
India
Myanmer
Thailand
1
2
3
4
5
6
7
8
9
10
11
12
13
14
15

figure1

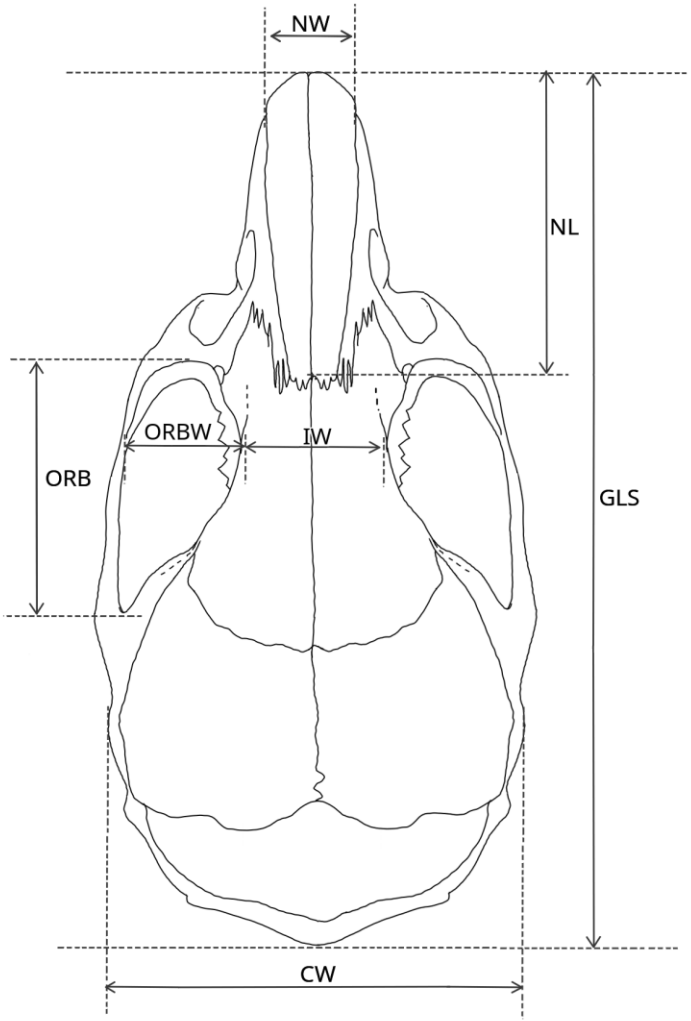
NW
NL
ORB
ORBW
IW
GLS
CW

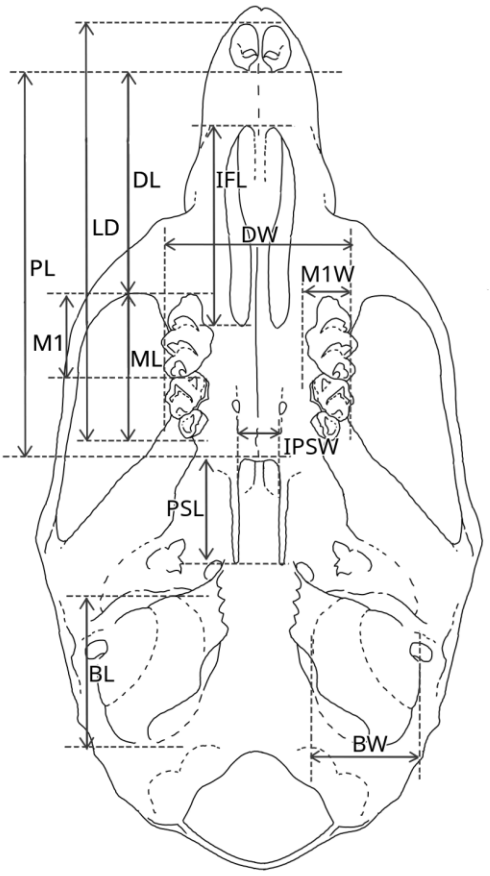
DL
IFL
LD
DW
PL
M1W
M1
ML
IPSW
PSL
BL
BW

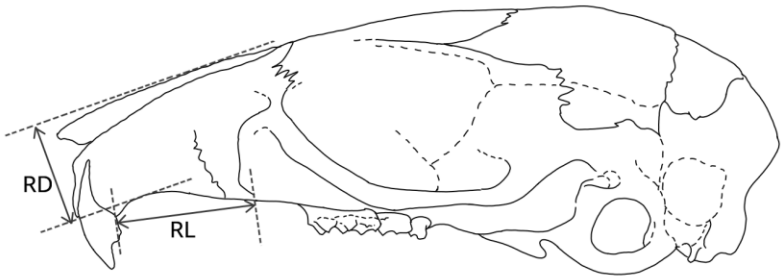
RD
RL

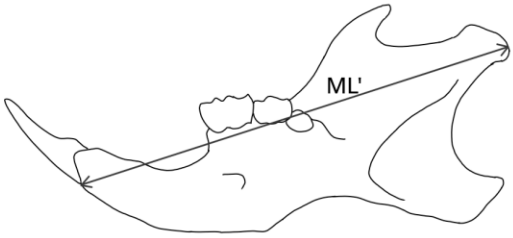
ML'

figure2

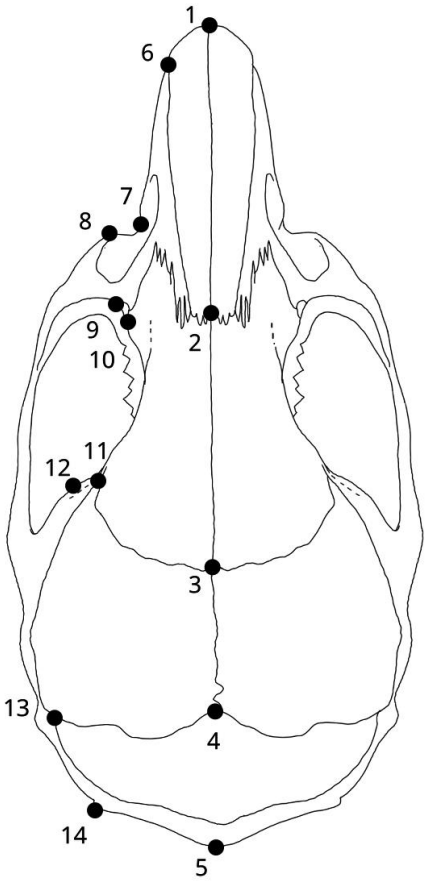

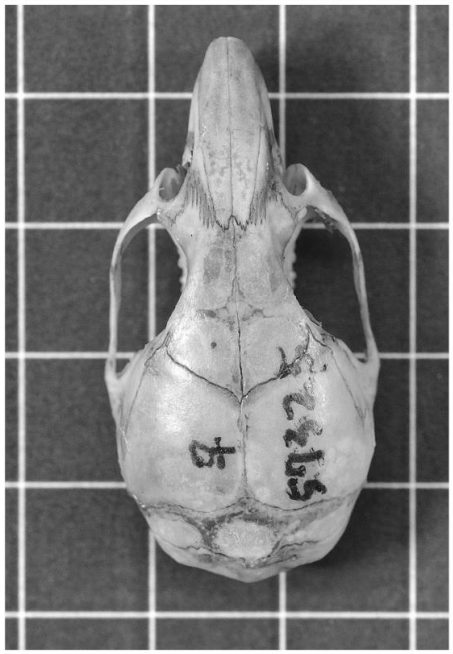

figure3

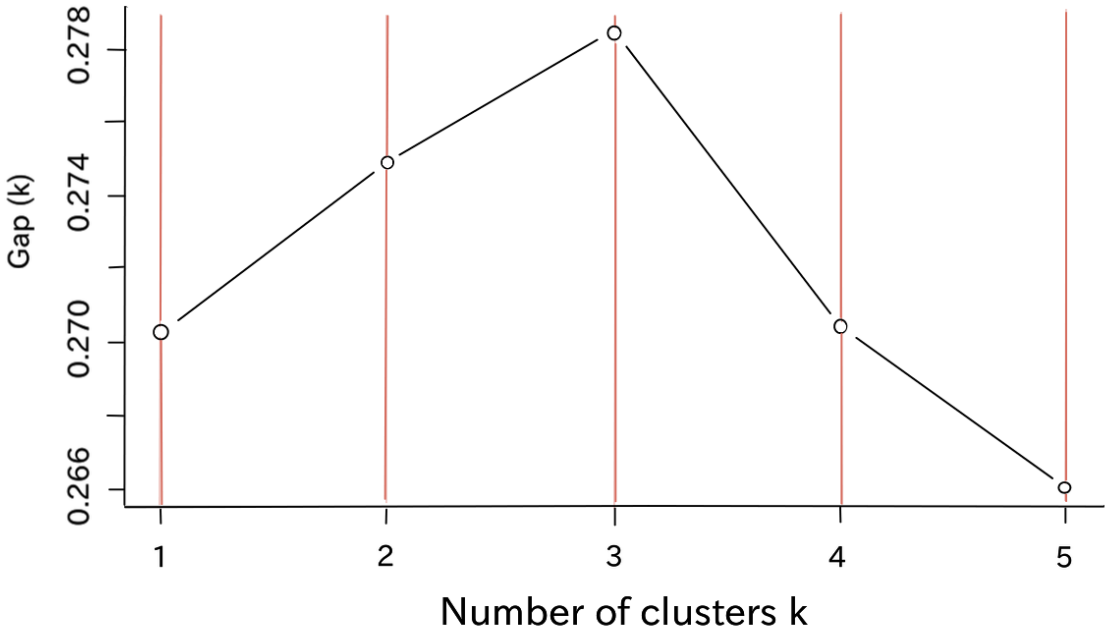

figure4

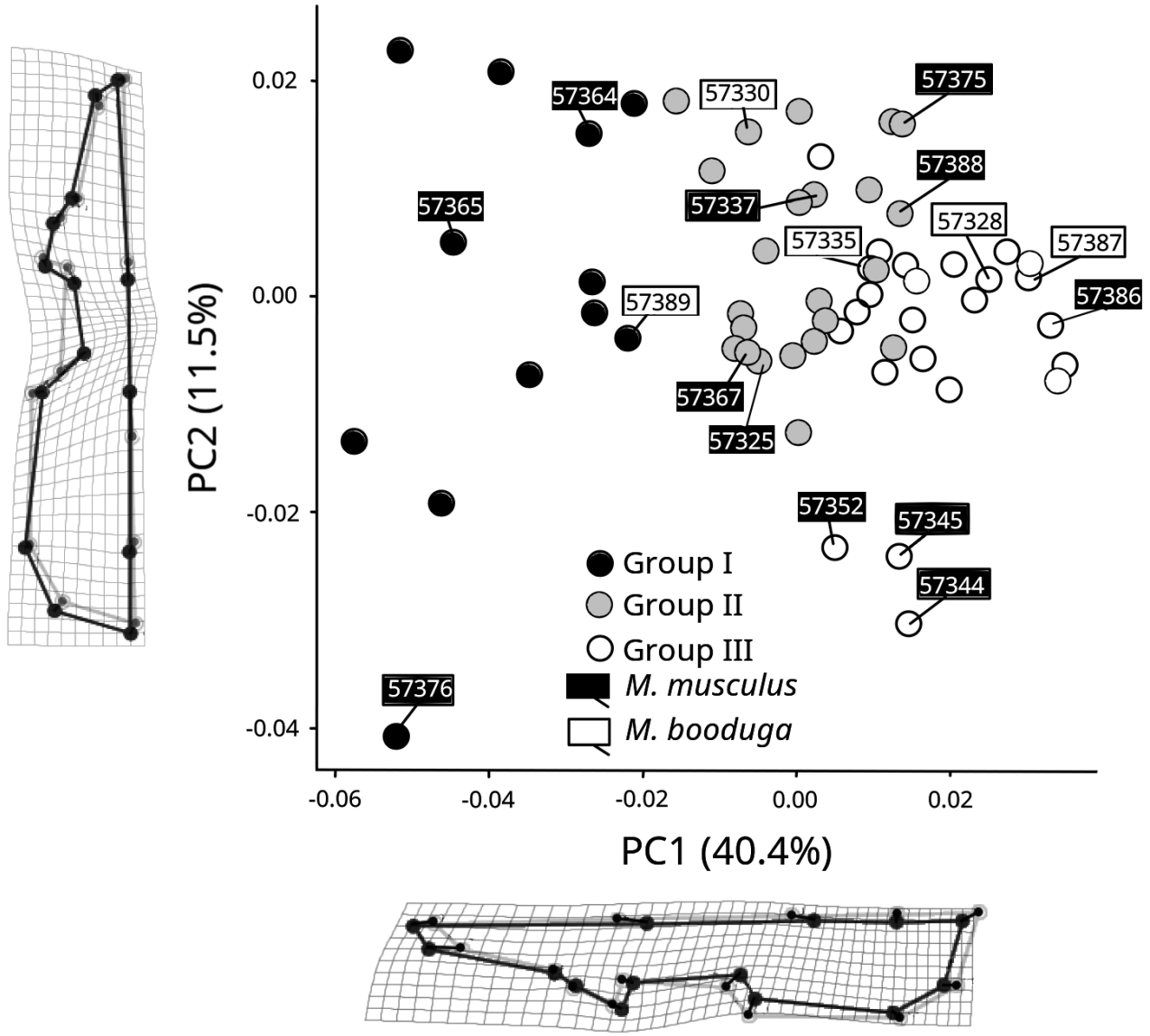

Fig. 3

figure5

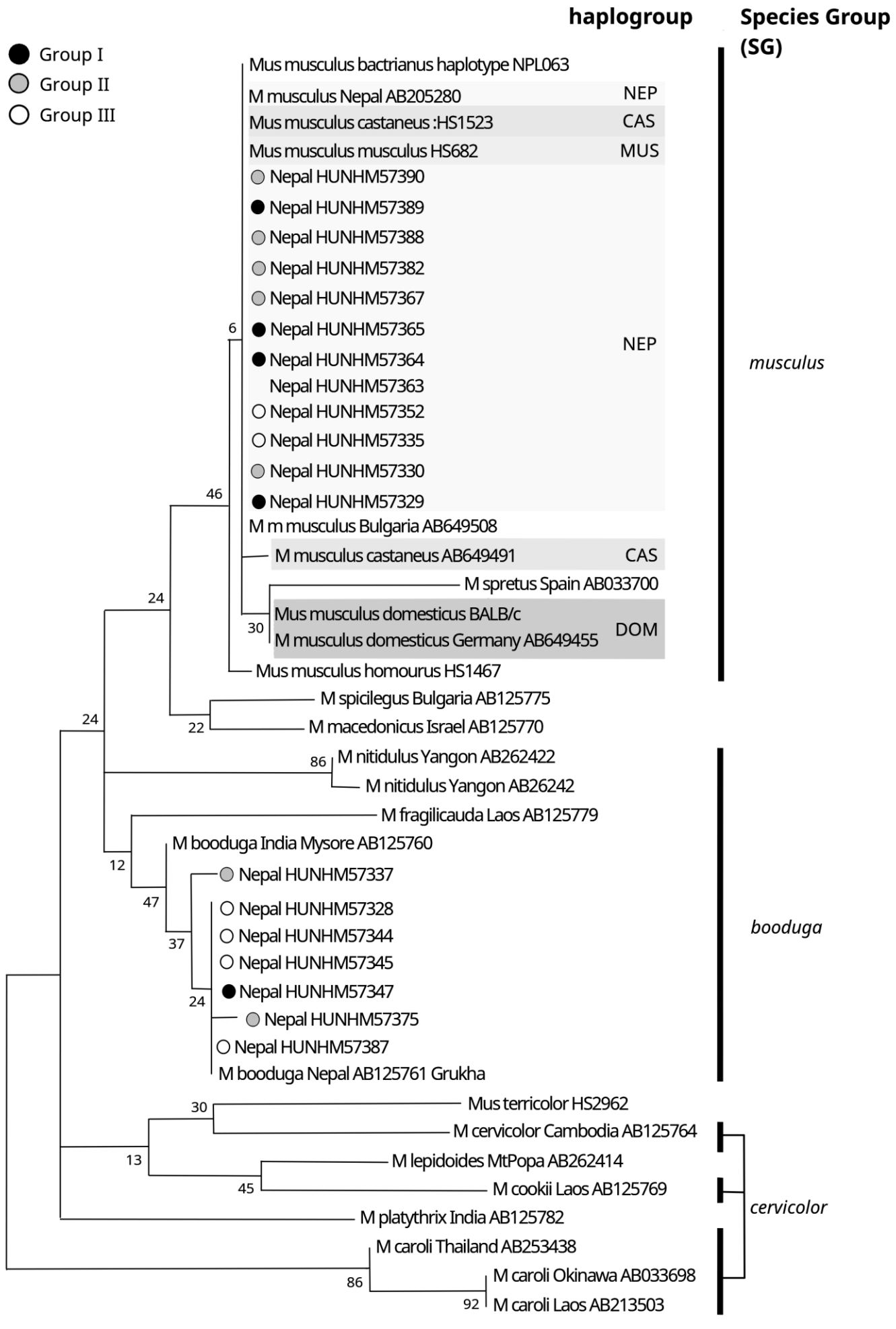
haplogroup
Species Group (SG)
Group I
Group II
Group III
Mus musculus bactrianus haplotype NPL063
M musculus Nepal AB205280
NEP
Mus musculus castaneus :HS1523
CAS
Mus musculus musculus HS682
MUS
Nepal HUNHM57390
Nepal HUNHM57389
Nepal HUNHM57388
Nepal HUNHM57382
Nepal HUNHM57367
Nepal HUNHM57365
Nepal HUNHM57364
Nepal HUNHM57363
Nepal HUNHM57352
Nepal HUNHM57335
Nepal HUNHM57330
Nepal HUNHM57329
NEP
musculus
6
46
M m musculus Bulgaria AB649508
M musculus castaneus AB649491
CAS
M spretus Spain AB033700
24
Mus musculus domesticus BALB/c
M musculus domesticus Germany AB649455
DOM
30
Mus musculus homourus HS1467
M spicilegus Bulgaria AB125775
24
22
M macedonicus Israel AB125770
86
M nitidulus Yangon AB262422
M nitidulus Yangon AB26242
M fragilicauda Laos AB125779
M booduga India Mysore AB125760
12
Nepal HUNHM57337
47
Nepal HUNHM57328
Nepal HUNHM57344
37
Nepal HUNHM57345
Nepal HUNHM57347
24
Nepal HUNHM57375
Nepal HUNHM57387
M booduga Nepal AB125761 Grukha
booduga
30
Mus terricolor HS2962
M cervicolor Cambodia AB125764
13
M lepidoides MtPopa AB262414
45
M cookii Laos AB125769
M platythrix India AB125782
cervicolor
M caroli Thailand AB253438
86
M caroli Okinawa AB033698
92
M caroli Laos AB213503
0.020

figure6

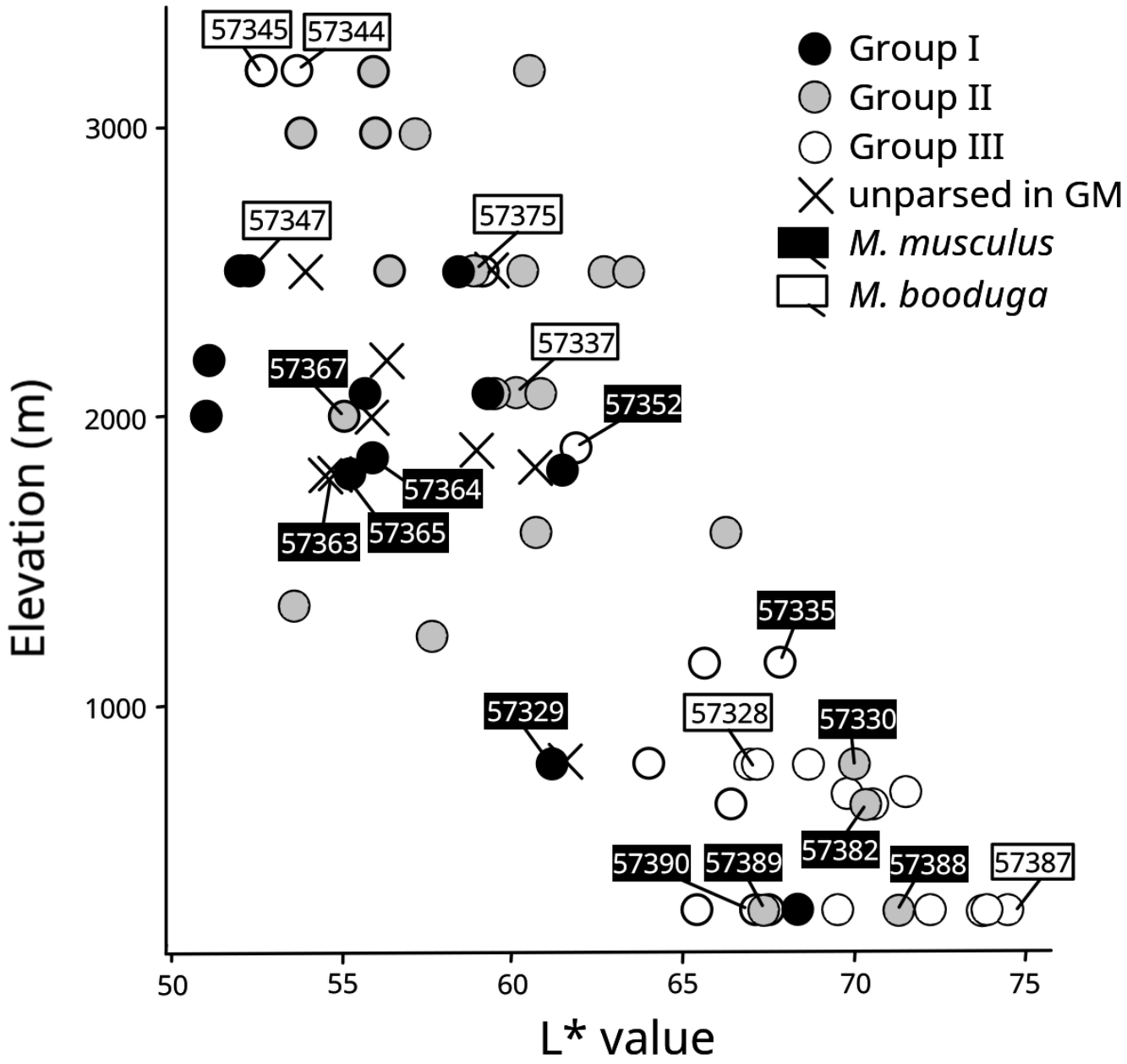
57345
57344
57347
57375
57337
57367
57352
57364
57363
57365
57335
57329
57328
57330
57382
57390
57389
57388
57387
Group I
Group II
Group III
unparsed in GM
M. musculus
M. booduga
Elevation (m)
3000
2000
1000
50
55
60
65
70
75
L* value

figure7

Table 1.List for the Abe Collection, including the information that we used here

(i.e., the collection sites, elevation, specimen number, sex, GLS, NL, L*, GM grouping number, and Cytb).

Map number and location		Elevation	HUNHM number	Sex	Linear measurements		Color	GM	Genotype	Accession
		(m)	specimens		GLS	NL	L*value	group	*Cytb*	number
1	Ghasa	2080	57337	♀	22.22	7.98	60.016	II	*M. musculus*	LC605038
			57338	♀	21.99	7.31	59.464	II	-	
			57339	♀	22.74	8.44	60.802	II	-	
			57340	♀	19.62	6.64	55.724	I	-	
			57341	♀	19.25	6.60	59.382	I	-	
2	Tatopani	1240	57336	♂	21.46	7.32	57.606	II	-	
3	Biratanti	1150	57335	♂	22.13	8.16	67.81	III	*M. booduga*	LC605037
		1150	57342	♂	21.72	8.31	65.604	III	-	
4	Pokkara	800	57328	♂	21.40	8.29	66.932	III	*M. booduga*	LC455568
		800	57329	♀	19.83	7.43	61.146	I	-	
		800	57330	♀	20.09	7.05	69.982	II	*M. booduga*	LC605036
		800	57331	♀	20.04	7.68	67.142	III	-	
		800	57332	♂	21.43	8.43	63.984	III	-	
		800	57333	♂	21.32	7.85	68.644	III	-	
		800	57334	♂	20.96	8.06	67.086	III	-	
		800	57343	♂	-	8.25	61.412		-	
5	Dhunche, Bagmati zone	2000	57366	♀	19.48	6.44	55.848		-	
		2000	57367	♀	22.22	7.49	55.062	II	*M. musculus*	LC455567
		2000	57368	♀	22.22	8.03	51.022	I	-	
6	syng Gonba, Gozainkund	3200	57344	♀	20.95	7.99	53.666	III	*M. musculus*	LC605039
		3200	57345	♀	20.41	7.32	52.612	III	*M. musculus*	LC605040
		3200	57373	♂	22.91	8.32	60.44	II	-	
		3200	57374	♀	22.20	7.98	55.918	II	-	
7	Syabru, Langtang	2200	57369	♀	19.22	6.53	51.074	I	-	
	Ghara Tabela, Langtang	2980	57370	♀	21.34	7.52	53.796	II	-	
		2980	57371	♀	22.28	7.66	55.926	II	-	
		2980	57372	♀	22.16	7.95	57.124	II	-	
8	Betrawate, Trisuli	700	57360	♂	21.10	7.91	69.782	III	-	
		700	57361	♂	23.85	9.75	71.462	III	-	
9	Khurumasang, Kathmandu	2500	57346		18.91	6.51	-		-	
		2500	57347	♀	19.10	6.75	52.286	I	-	
	Khurumasang, Helambu	2500	57375	♂	22.26	8.10	58.932	II	*M. musculus*	LC605043
		2500	57376	♂	18.80	6.20	58.414	I	*M. musculus*	LC605044
		2500	57377	♂	19.54	6.57	52.01	I	-	
		2500	57378	♂	18.24	5.05	53.926		-	
		2500	57379	♀	23.16	8.64	56.364	II	-	
10	Pati Bhanjyang, Kathmandu	1820	57348	♂	20.48	7.17	61.442	I	-	
		1820	57349	♂	-	7.48	60.608		-	
11	Kuinibisona, Kathmandu	1890	57352	♂	21.61	7.99	61.8	III	*M. musculus*	LC605041
12	Balaju River Banle, Kathmandu	1350	57327	♀	21.19	8.09	53.602	II	-	
	Sundarijal, Kathmandu	1890	57350	♂	-	-	58.944		-	
	Baneshwor, Kathmandu	-	57353	♂	-	-	61.366		-	
	Phulchowki, Kathmandu	2200	57354	♂	-	7.17	56.33		-	
		2500	57355	♀	20.78	6.45	59.326		-	
		2500	57356	♂	21.77	8.11	59.158	III	-	
		2500	57357	♂	21.44	8.00	62.652	II	-	
	Sheopuri, Kathmandu	2500	57358	♀	21.74	7.97	63.356	II	-	
		2500	57359	♀	22.40	8.34	60.298	II	-	
	Ramache, Kathmandu	1800	57362	♂	21.93	8.11	54.586		-	
		1800	57363	♀	-	-	54.736		*M. musculus*	LC455566
		1850	57364	♀	21.06	7.77	55.902	I	*M. musculus*	LC455570
		1800	57365	♂	19.08	6.67	55.184	I	*M. musculus*	LC605042
13	godavari, kathmandu valley	1600	57325	♀	20.53	6.78	60.722	II	*M. musculus*	LC605035
	godavari, Kathmandu	1600	57326	♂	20.85	7.14	66.232	II	-	
14	Hitaura, Bhainse	660	57380	♂	22.54	8.19	70.564	III	-	
		660	57381	♀	21.40	8.06	66.436	III	-	
		660	57382	♂	20.56	7.56	70.356	II	-	
15	Adhabar, Terai	300	57351	♂	19.93	7.05	67.466	II	-	
		300	57383	♀	20.58	7.88	67.1	III	-	
		300	57384	♂	20.88	7.98	69.554	III	-	
		300	57385	♀	21.31	8.47	69.518	III	-	
		300	57386	♀	22.92	9.46	73.746	III	*M. musculus*	LC605045
		300	57387	♂	22.82	8.72	74.474	III	*M. booduga*	LC455569
		300	57388	♂	21.69	8.04	71.282	II	-	
		300	57389	♀	19.02	6.77	68.346	I	*M. booduga*	LC605046
		300	57390	♀	20.49	7.78	67.356	II	-	
		300	57391	♂	21.67	8.33	72.254	III	-	
		300	57392	♂	22.04	8.46	73.904	III	-	
		300	57393	♂	21.20	8.10	65.334	III	-	
		300	57394	♂	20.66	7.64	69.54	III	-	

Table2 List of the socores in comparison of mean measurement scores among category (See Supplementary Data SD2 for abbreviations.)

(X ± SD)

	category		GLS	NL	CW	B+H	L (ventral)	HB/TL	NL-GLS/4	GLS/CW	NL/GLS	Centroid size
Abe collection	Partial molecular analyses	*M. musculus* (n = 11)	20.73 ± 1.20	7.50 ± 0.52	9.43 ± 0.33	77.45 ± 9.62	62.87 ± 6.86	1.07 ± 0.08	2.31 ± 0.30	2.20 ± 0.09	0.36 ± 0.01	1722.54 ± 94.50
		M. booduga (n = 7)	21.31 ± 1.28	7.88 ± 0.65	9.56 ± 0.23	79.71 ± 9.30	59.85 ± 8.29	1.06 ± 0.10	2.55 ± 0.38	2.23 ± 0.10	0.37 ± 0.01	1777.25 ± 101.98
	GM Groups besed on shape	I (n = 12)	19.77 ± 1.01	6.93 ± 0.55	9.35 ± 0.26	69.83 ± 6.44	56.83 ± 5.20	1.04 ± 0.07	1.99 ± 0.34	2.12 ± 0.13	0.35 ± 0.01	1623.23 ± 54.61
		II (n = 23)	21.65 ± 0.90	7.76 ± 0.49	9.69 ± 0.39	83.09 ± 7.18	61.08 ± 5.40	1.09 ± 0.08	2.35 ± 0.35	2.23 ± 0.05	0.36 ± 0.01	1800.07 ± 71.72
		III (n = 24)	21.53 ± 0.87	8.21 ± 0.52	9.45 ± 0.30	78.79 ± 5.56	67.00 ± 5.62	1.10 ± 0.10	2.83 ± 0.35	2.28 ± 0.07	0.38 ± 0.01	1793.99 ± 71.92
outgroup		*M. booduga* (n = 2)	19.40 ± 0.49	7.59 ± 0.13	8.81 ± 0.23	67.50 ± 2.12		1.22 ± 0.05	2.74 ± 0.01	2.20 ± 0	0.39 ± 0	
		M. musculus (n = 19)	20.04 ± 1.30	7.08 ± 0.60	9.39 ± 0.40	72.00 ± 7.32		1.22 ± 0.13	2.07 ± 0.33	2.13 ± 0.08	0.35 ± 0.01	
		M. cookii (n = 3)	25.24 ± 0.21	9.73 ± 0.50	10.54 ± 0.18				3.42 ± 0.49	2.40 ± 0.05	0.39 ± 0.02	
		M. caroli (n = 2)	20.39 ± 1.13	6.96 ± 0.41	9.35 ± 0.50	93.00		1.01	1.86 ± 0.13	2.18 ± 0	0.34 ± 0	